Design and Test of an Electromechanical Rover Tether for the Exploration of Vertical Lunar Pits

Patrick McGarey, Tien Nguyen, Torkom Pailevanian, Issa Nensas
Jet Propulsion Laboratory,
California Institute of Technology
4800 Oak Grove Dr.
Pasadena, CA 91103
***first.last*@jpl.nasa.gov**

***Abstract*—Moon Diver is a proposed mission to land and deploy an extreme-terrain, tethered rover for the exploration of Tranquillitatis Pit, a large vertical cave entrance into the subsurface of Earth's Moon. By leveraging a supportive tether, the Axel rover, developed by NASA's Jet Propulsion Laboratory, would perform a controlled descent into the pit and deploy instruments along the pit wall. The purpose of this mission concept is to study a volcanic secondary crust as a function of depth in order to determine formation processes and chemical makeup. The lifeline of the mission would be the tether, which provides power from, and communication to the top-side lander. Critically, the tether also serves as mechanical support between the suspended rover and the lander, which acts as an anchor. While space tethers have been deployed both in orbit and terrestrially, the use of the proposed tether is unlike any known in the literature; the tether must come into contact with the terrain while under load. With respect to the environment, the tether must also survive abrasion from glassy regolith and volcanic rocks, bending around sharp edges, thermal extremes, and exposure to full spectrum ultra-violet (UV) radiation, all while reliably transferring up to 100 W of power and 1 Mbps of data. Furthermore, since the Axel rover pays out tether from an internal spool, the tether's diameter must be minimized to increase spool capacity, allowing for up to a 300-m traverse while also meeting static and dynamic strength requirements. This paper covers several phases of the tether's initial development, including i) a trade study of structure and materials with consideration for space heritage, ii) selected design justification, and iii) results from tests on prototype tethers looking into mechanical, electrical, and environmental properties, including exposure to rock-regolith abrasion, load profiles at temperature, and degradation due to UV exposure while exposed to vacuum. Finally, we provide insights and lessons learned from lab and field tests, which inform our continued effort to design a tether capable of surviving rugged, lunar conditions.**

TABLE OF CONTENTS

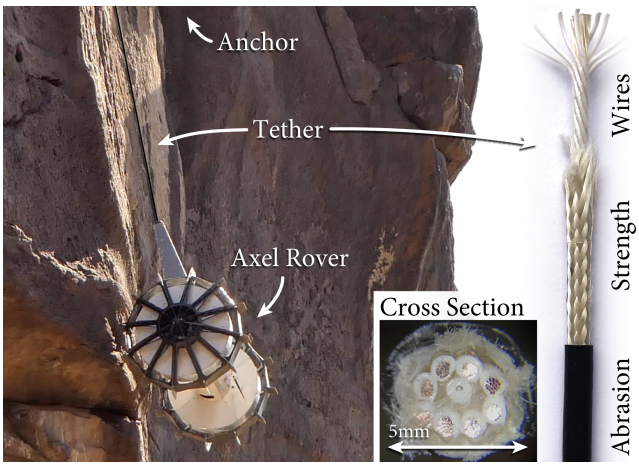

Figure 1: The Axel rover is shown during a field test supported by a custom, electromechanical tether.

1. INTRODUCTION

For decades, mobile robots have been sent to explore the surface of distant planetary bodies, often favoring flat, benign terrain in order to ensure the safety and longevity of the system. However, some of the most interesting science targets are located on steep terrain, e.g., craters, lava tubes, and pits, which offer direct clues into the formation history of the planet and our solar system, but are out-of-reach for current rovers. One mission concept, which would explore below the surface of another body for the first time, is Moon Diver, a proposed NASA Discovery mission to deploy a tethered rover down a vertical, lunar pit in order to investigate emplaced lava layers as a function of depth and confirm the existence of a potential subsurface lava tube [1], [2]. Our target is Tranquilitatis Pit, which was discovered by the Japan Aerospace Exploration Agency (JAXA) in 2009 [3], and imaged by NASA's Lunar Reconnaissance Orbiter (LRO) in 2012 [4]. Studies have determined that this pit is roughly 100 m in diameter and up to 125 m deep. This mission would be critical to understanding both the formation history and chemical makeup of Earth's Moon from vertical layers that are intact and chronologically in order, as opposed to shredded apart and mixed up as you would find on the surface as regolith. The enabling technology for this mission is Axel, a simple, two-wheeled, tethered rover developed and matured by NASA's Jet Propulsion Laboratory (JPL) in collaboration with Caltech [5], [6]. The lifeline of the mission concept is the supportive tether, which also provides wired power and

© 2018. California Institute of Technology. Government sponsorship acknowledged

communication to a lander stationed on the surface and acting as an anchor for the rappelling system. The literature provides many examples of 'space' tethers for use in orbital applications, but for the first time, a tether is proposed that would come into contact with the terrain while under appreciable load. This paper focuses on the development, design, and testing of a 'terrestrial' tether that can withstand the harsh lunar environment and terrain while supporting and meeting critical mission requirements of mechanical support, power throughput, and communication bandwidth. Specifically, we address the trades involved with designs suited for the environment, building a tether, and testing to assess mechanical and electrical properties.

The remainder of this paper is organized as follows. Section 2 summarizes prior work on tether applications for space missions. Section 4 presents a detailed trade study and selected design parameters for the lunar tether. Section 5 offers results from a series of tests performed under relevant conditions with different tether prototypes. Section 6 provides concluding marks and future work.

2. Related Work

Space tethers have been an active area of interest for decades, starting with the Gemini missions in the late 1960s. Initially, tethers were used to demonstrate in-orbit capabilities around Earth, where topics of interest included dynamic analysis of weightless tethers, formation flying of satellite systems, momentum exchange, electrodynamics, and plasma physics [7]. The Tethered Satellite System (TSS) deployed the longest ever tether, measuring 20 km, which was launched from the Space Shuttle [8]. Unfortunately, a failed wire insulation caused an arc, severing the tether after deployment. Tethers have also been employed in the exploration of terrestrial bodies like Earth's Moon and Mars. During the Apollo Program, astronauts on several missions deployed a Surface Experiments Package (SEP), which involved a host of instruments, all linked to a central station via discrete flex print cables [9]. Although these tethers were not loaded, they did come into contact with the lunar surface. These tethers represent the first use of terrestrial tethers.

On Mars, tethers have been used to support communications for JPL's Curiosity rover prior to separation from the decent stage [10], and recently, as supportive umbilicals for the InSight lander's seismometer and subsurface drill [11]. Still, these tethers differ in function from how they are used with tethered rovers as the cable does contact the terrain under appreciable tension, i.e., supporting the static and dynamic loads of a rover on sloped or vertical terrain. Tethered rovers, have been a topic of research interest for several decades. In the 1990s, the first steep-terrain, tethered rover was fielded in the exploration of volcanic craters [12]. Starting in the early 2000s, JPL began to develop tethered rover systems [13]. A detailed history of tethered rovers can be found in [14]. The Axel rover, developed at JPL, is a two-wheeled rover with an articulated tether boom and instrument bay capable of storing and deploying full-sized science instruments to make co-located measurements on the surface regardless of its slope. The Axel rover stores and pays out tether from an internally actuated tether spool as shown in Figure 2. A common approach for terrestrial tethered rovers in the literature is to use off-the-shelf, electromechanical tethers tailored for underwater environments or oil and gas applications. Such tethers feature a common construction made of internally wound wires, an over-wrapped strength braid made of high-strength fiber strands, and an outer sacrificial layer to limit abrasion of the strength material and damage to internal conductors. This design will serve as the basis for the design trade referenced in the remainder of this paper.

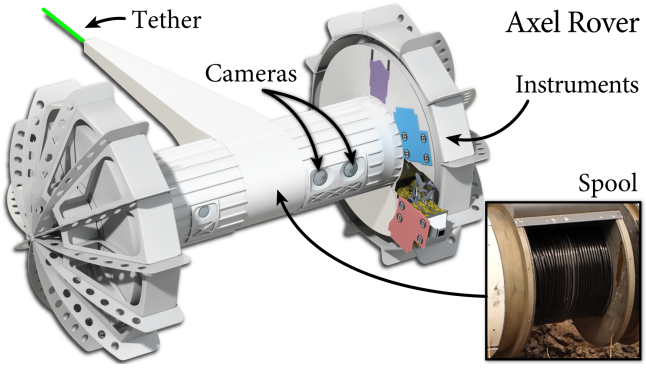

Figure 2: *Axel Rover*: The main components of the rover are identified along with a picture of tether spooled around the central body. There are five degrees of freedom in the Axel system, one for each wheel, one for the central body, one for the tether deployment boom, and one for the tether spool.

3. Tether Requirements

A critical function in the design of a terrestrial tether is to understand the constraints levied by both the environment and the terrain. The following list provides notional requirements for tethers that should generally be considered regardless of the targeted terrain. These requirements can then be associated to both the lunar environment and proposed mission timeline. The Moon Diver mission concept proposes a one-way, one lunar day operation that lasts just 14 Earth days or one half of a lunar cycle. As such, we can constrain the expected surface/pit temperatures by thermal modeling to be within -50 C to 150 C, peaking at lunar noon. With respect to the terrain, we are challenged by the presence of abrasive regolith in our approach to the pit, and sharp basalt rocks transitioning from the regolith to the steep pit walls. Additionally, the Moon is an airless body, so the effects of solar radiation and ultra-violet (UV) exposure must be considered for the duration of the proposed mission, as UV degradation is known to be exacerbated in vacuum environments.

Requirement	Detail
Loading	Support rover static and dynamic loads
Bending	Survive bending around obstacles
Abrasion	Survives expected cyclic contact with terrain
Thermal	Materials are rated for temperature extremes
Radiation	Survive exposure to radiation environment
Vacuum	Survive exposure to total vacuum
Impacts	Survive impacts from tumbling objects
Pinching	Survive snagging or pinching in rock or crevice
Twisting	Robust to damage from torsional strain
Memory	No critical deformation when stored on spool

Table 1: *High-Level Tether Requirements.*

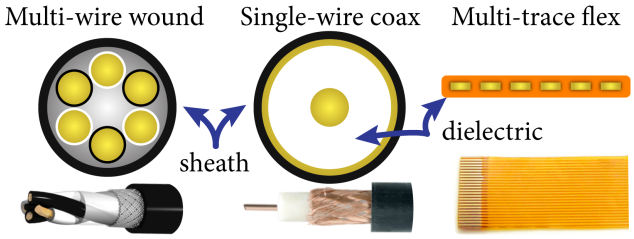

Figure 3: *Tether Cross Section*: Three prime geometries for tethers are shown. Gold/yellow colors represent conductors.

4. Design

What follows is a summary of a trade study conducted for a lunar tether design that considers tether structure, materials, and electrical transmission properties. For each topic, we expand on available options, listing advantages/disadvantages and recommend an approach that would meet both mission and environmental constraints.

Tether Structure:

The structure of an electromechanical tether considers three primary architectures: wound, coaxial, or flat, multichannel flex. The cross-sectional design for each architecture is shown in Figure 3. The following table assigns a '+' or '-' for different performance metrics related to the cross-sectional design of a tether.

Metric	Wound	Coax	Flex
Strain Relief	+	-	-
Load Path	+	+	-
Spool Capacity	+	+	-
Bend Resistance	+	+	-
Redundancy	+	-	+
Noise Immunity	-	+	-
Totals	5	4	1

Table 2: *Cross-Sectional Performance Metrics*: Strain relief considers resilience to stretching under tension, the load path concerns how tensile stress can deform a tether, spool capacity considers packing density and efficiency (circular geometries can be stored on a spool with multiple wraps and rows), bend resistance considers susceptibility to damage when bent around a small radius, redundancy considers if spare wires can be accommodated, and noise immunity considers wire shielding for noise attenuation.

The wound cable architecture out performs other choices with respect to the chosen metrics because the helical winding of internal conductors is best suited for a tether that will be loaded and stretched. Furthermore, although the noise immunity is better for coaxial and flex cables (assuming a shield is used), measures can be taken to limit the noise of a wound cable by helically winding wires, adding an external braided shield, or limiting the number of wire to achieve a 'star-quad' geometry, which has performance characteristics approaching that of twisted wire pairs [15]. Twisting individual pairs of wires (like an Ethernet cable) was not considered as it complicates the packing geometry and is not ideal for loading and elongation. An advantage of the helically wound design is that fiber-optic lines can easily be passed through the center of a wound cable for redundant and fast communication (Section 4 discusses the communication trade in more detail).

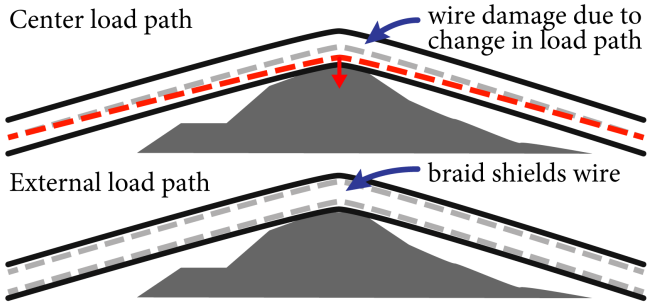

Figure 4: *Load Path*: A center load path includes strength members passing through the tether's core. An external load path includes over-braid structures that distribute loads uniformly when compressed.

The selection of a wound-wire geometry leads directly into the selection of the load path, which involves consideration for the environment that the tether will come into contact with. In this case, we expect the tether to contact both regolith and rocks as part of the nominal mission. Therefore, the load path is selected to avoid damage to the tether internals when it is in contact and under load. Figure 4 demonstrates why a central load path, which is usually the correct approach in lifting applications, is not ideal for a cable that is laid on the surface and put in tension; the central strength member will cut into the lower wires when loaded potentially causing damage. Instead, an external, over-braided, strength layer is preferred for its ability to distribute loads more evenly and protect the internal conductors.

Figure 5: *Strength Layer*: Example structures/geometries.

Figure 5 illustrates different geometries that can be implemented in a tether to achieve tensile strength. Strings, made of individual filaments or fibers, offer strength when woven or braided, which improves both robustness and elongation properties. Cables are helically wound metal wires that are incredibly strong and used for hi-load applications (e.g., bridge suspension wires) but have a high mass per unit length and will foul if twisted in the opposite direction. Braids of high-strength fibers provide excellent tensile strength and redundancy (a factor of string quantity) as well as improved elongation properties (a factor of the Poisson ratio which directly related to braid geometry). Braids falls into three subcategories – single-braid, over-braid, and three-dimensional braids. Single braids are similar to ropes and create a center load path, over braids are hollow and compress laterally as they are loaded, which enables an external load path, while 3D-braids are layered over braids often paired with composites to make pressure vessels for aerospace applications. An over-braid geometry is selected for this design since it is both strong and accommodates an external load path. An exotic approach is to use lattice structures, e.g., carbon nanotubes, but this approach is not currently used because few products exist at appreciable lengths (beyond those used in lab settings).

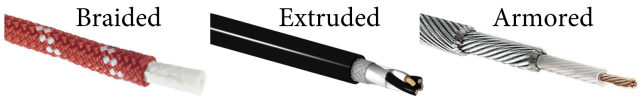

Figure 6: *Abrasion Layer*: Approaches for resisting environment abrasion on a tether, cable, or rope are shown.

The abrasion layer is the outer-most layer of a tether, which can be omitted in certain environments where abrasion and UV degradation are not a concern. However, for lunar applications, the abrasion layer is critical in minimizing damage to the strength layer by 1) micron-scale, 2) jagged, regolith particles, which embed and shred fibers, and 3) strong UV, which can decrease the tensile strength of fibers over time. Figure 6 shows common approaches to limit abrasion in tethers. Braided jacketing is often used in climbing applications as a wearable layer called a *kernmantle*. The braid is a floating layer that allows the strength material and wires to move beneath. One limitation of a braided jacket is that it cannot completely prevent small particles from entering. Instead, an extruded jacket can be considered, which is deposited over the strength layer and provides full protection from moisture, UV, and small particles. One disadvantage of an extruded jacket is that it typically decreases the overall flexibility of the cable and will buckle when severely bent. An armored approach, offers supreme protection from abrasion but it not considered because it involves heavy strands of wire, which make the cable extremely stiff and thus, difficult to store in a small volume.

Figure 7: *Selected Tether Structure*

The selected cross-sectional design, load path, strength, and abrasion layers are illustrated in Figure 7. We note that the fill layer can accommodate either non-loaded fiber reinforcement or even fiber-optic strands for communications. The layer thicknesses are notional and will be constrained later by material selection.

Tether Materials:

In selecting appropriate materials for the tether we consider the lunar environment and prior uses of that material in space. Figure 8 provides a detailed trade table showing options for each layer, including insulator wrap on conductors, conductors, strength, and abrasion layers. The rows of the table are grouped by layer and the columns show properties of the material determined from vendor data and available NASA documentation. One difficulty with assessing materials is that properties can vary from manufacturer to manufacturer, so this list represents a best effort by the authors to combine a large amount of information for a comparative evaluation and should not be considered definitive.

Starting at the tether's center and moving outward, we use a filler of high-strength Vectran fiber, which support the cable geometry during compression. Multi-strand (40), 28 AWG copper wires are selected for bend resilience and their capabilities of transmitting power/data using the same wire construction. Section 5 will provide more detail on gauge selection. Teflon insulation, more specifically FEP, is selected for its excellent high temperature resistance, low outgassing properties, and flexibility. Kapton is commonly used in conjunction with Teflon insulation to provide layered insulation, but that approach was not used here to reduce complexity but may be revisited for the flight version of the tether. There are numerous possibilities to consider for the braided strength layer. Not only are there many high-strength fiber variants (polyarylate, polyethylene, polyamide, polybenzoxazole, etc.) but there are also conductive fiber variants. Vectran (polyarylate) is selected for its low density-to-strength ratio, high-temperature performance (lunar noon reaches 150 °C), low creep/expansion, and most importantly, high bend strength (ideal for experiencing knife-edge bends under load). While Zylon has better strength and thermal properties, it has higher CTE and moisture absorption than Vectran, which is already sufficient given the load requirement. Lastly, an extruded Tefzel jacket is selected as the abrasion layer. Tefzel (ETFE) has good temperature properties, mass, and excellent abrasion resistance. For testing purposes, three prototype tethers were produced, each with a varying jacket type to evaluate the performance of braided vs. extruded and extruded Tefzel vs. Nylon 11. We note that Tefzel has better high-temperature properties than Nylon but involves a longer fabrication time because Tefzel requires a specialized extrusion process.

Electrical:

The mission concept of Moon Diver involves a lander serving as an anchor, power source, and communication relay back to Earth. By transmitting power through the tether, the rover can continue to operate in the darkness of the pit by leveraging solar power generated on the lander. With respect to communications, the rover would be beyond line-of-sight to lunar orbiters and Earth, so critical data and telemetry would be relayed back to the lander via the tether. The tether design must account for power transmission losses and voltage drop given the 300-m tether length. Accordingly, the following table trades alternating vs. direct current transmission.

	DC	AC
Conductors	(+) 2 conductors (requires fewer spares). (+) 2-conductor DC is more efficient over long lengths than 2-conductor AC.	(-) 3 conductors (requires more spares). (-) 2-Phase is less efficient.
Inductance	(+) Not significant but occurs over long wires, about 1 uH/m.	(-) Potentially large for spooled wire due to high impedance, which changes as tether is paid out, meaning that frequency tuning may be necessary.
Losses	(-) Stepping up voltage reduces I^2R losses but requires step/down converters that are less efficient than AC transformers.	(-) Losses are increased via skin effect and requires potentially lower frequencies to mitigate, which can result in issues with interference and inductance.
Support	(-) Step-up/down converters are needed for high-voltage long-range transmission, heritage for step-down is low (Commercial solutions are prone to single-event latch up).	(+/-) Would require single passive rectifier and transformer, which is simple solution but these devices are large in volume and mass.

Table 3: *Power Transmission*: DC is preferred over AC due to better 2-wire efficiency and lower inductance from spooling.

		Density (g/cm3)	Strength (GPa)	Modulus (GPa)	Critical Temp (C)	Elongation	Outgassing	Moisture Regain	Bend Strength	Conductivity	UV Resistance	Space Heritage	Examples
Ins + Wrap	Teflon (PTFE or FEP)	2.2	0.0	1	204	300%	0%	0%	High	Low	High	High	Many: Wire Ins
	Kapton	1.4	0.2	3	260	72%	1%	2%	Mod	Low	High	High	Many: Wire Ins
Pwr/Data	Fiberoptic	2.2	1.4	16	1000	2%	1%	0%	Low	Low	Mod	High	ISS
	Metal Clad Fiberoptic	5.1	0.6	16	600	2%	1%	0%	Low	High	High	Low	n/a
	Copper	9.0	0.2	117	760	20%	0%	0%	High	High	High	High	All Missions
Strength + Pwr/Data	Conductive: Aramid (Aracon)	3.0	2.9	83	200	3%	1%	1%	Mod	High	Low	High	TEPCE
	Conductive: Vectran (Liberator)	3.0	3.0	75	200	4%	1%	0%	High	High	Low	Low	n/a
	Conductive: Zylon (Amberstrand)	3.6	5.8	180	250	3%	1%	1%	High	High	Low	Low	n/a
Strength	Polyarylate: Vectran	1.4	3.2	75	200	4%	1%	0%	High	Low	Low	High	MER, MSL
	Polyethylene: Dyneema	1.0	3.4	113	70	4%	1%	0%	High	Low	Mod	High	Shuttle
	Polyethylene: Spectra	1.0	3.3	124	70	3%	1%	0%	High	Low	Mod	High	Shuttle
	Polyamide: Technora	1.4	3.0	70	200	4%	1%	2%	High	Low	Mod	High	MER, MSL
	Polyamide: Twaron	1.4	2.4	60	200	2%	1%	5%	High	Low	Low	Low	n/a
	Polyamide: Aramid (Kevlar)	1.4	3.6	83	200	4%	1%	6%	Mod	Low	Low	High	TSS-1R
	Polybenzoxazole: Zylon	1.7	5.8	180	250	3%	1%	1%	High	Low	Low	High	MER, MSL
	E-Glass	2.6	2.0	72	346	5%	0%	0%	Low	Low	Mod	High	ISS, Space Suits
	Carbon Fiber	1.8	4.3	228	300	2%	0%	0%	Mod	Mod	High	High	MSL, Maven, Orion
Abrasion	Extruded: Nylon 11 (PA 11)	1.1	0.0	1	150	10%	0%	0%	High	Low	Mod	Low	n/a
	Extruded: Tefzel (ETFE)	1.7	0.0	1	200	300%	0%	0%	High	Low	Mod	High	Many
	Extruded: Teflon (PTFE)	2.2	0.0	1	204	300%	0%	0%	High	Low	High	High	Many
	Braided: Polyester: Dacron	1.4	1.1	15	150	13%	1%	0%	High	Low	Mod	High	Space Suits
	Braided: Nomex	1.1	0.5	8	370	4%	2%	6%	High	Low	Mod	High	TSS-1R, Heat Shield
	Braided: Aluminosilicate (Nextel)	2.8	1.6	150	700	2%	0%	0%	Mod	Low	High	High	Heat Shield

Figure 8: *Materials Trade*: This table shows materials commonly used for tether components, including conductor insulation or wrap, conductors, strength, and abrasion layers. We note that some strength materials and even fiber-optic strands can double as conductors. Colors are assigned to cells based on favorability. Unfavorable values are the most red, favorable values are the most green, and moderate values are yellow. Any cells that are opaque are not relevant metrics for comparison. The color scheme resets for rows separated by thick black lines so that the color gradient only applies to one particular layer of the tether. Materials selected for the lunar prototype are identified by a green highlight.

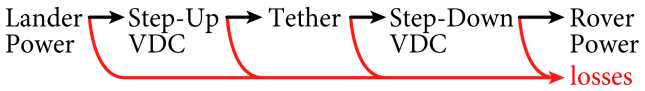

Figure 9: *Power Transmission Path*: This illustration shows the pathway starting from the lander (generating solar) and ending at the rover after efficiency and heating losses.

As illustrated in Figure 9, the transmission path flowing from the lander to the rover involves losses. Losses correspond to the relationship, $Loss = I^2R$, where I is the current and R is the two-way (send/return) resistance at the highest expected temperature, i.e., 150 °C, for a pair of wires of known length. The baseline tether length for the mission concept would be 300 m. Since the maximum expected continuous power required by the rover is 34 W, we use high voltage to limit heating losses in the tether. A simple power calculation can be done to calculate component losses considering the path shown in Figure 9. Figure 10 shows how voltage increases reduce the power input from the lander and increase available rover power.

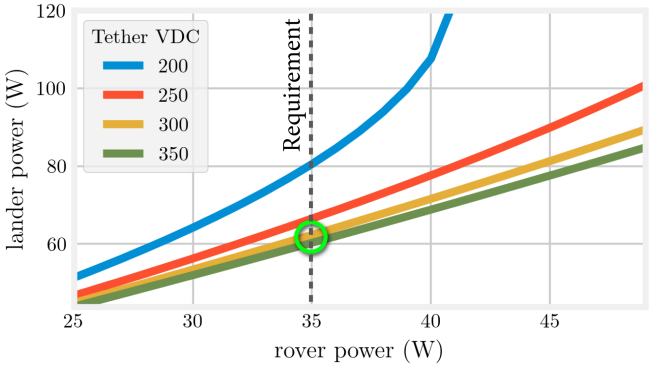

Figure 10: *Lander vs. Rover Power*: The plot shows the result of a power calculation, assuming losses on a single 28 AWG wire pair, that determines how much lander power is required to produce rover power for different voltage levels. As shown, voltages less than 300 VDC cannot provide enough power due to line losses and heating.

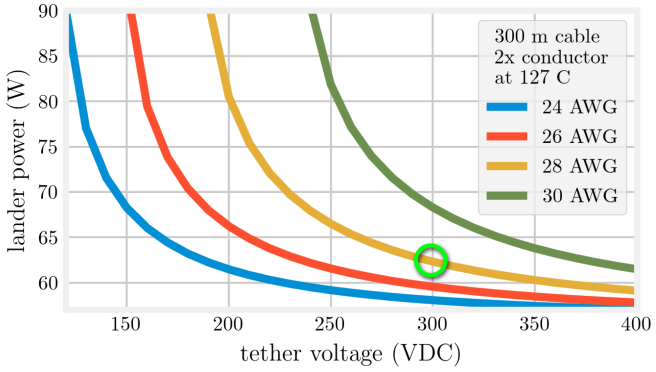

Figure 11: *Lander Power vs. Tether Voltage*: This plot offers a different take on Figure 10, showing voltages necessary to produce 34 W on the rover side for different wire diameters assuming a single pair.

In Figure 11, we see the impact of wire gauge selection and voltage for 34 W of power transmission through a 300-m tether. Due to available step-down power conversion approaches with space heritage, we limit the upper end voltage to be within 300-350 VDC (300 VDC is the current baseline). This approach allows for the use of a stacked fly-back converter topology to step up from a 32 VDC, nominal lander voltage to a 300-VDC tether voltage, and later, step down to the rover's operating voltage of 28 VDC. Figure 12 plots the power distribution of 62 W into the system assuming that just one wire pair is used. As shown, to arrive at 34 W for the rover, 6 W are used for 'house-keeping' power, i.e., small losses from power distribution modules on the lander side, 15 W are used in step up/down conversion losses (assuming an 85% efficiency), and 5 W are lost through tether heating. We note that 34 W is the maximum expected continuous current. Accordingly, we expect all losses to decrease slightly from what is shown, especially if other spare wire pairs are still functional.

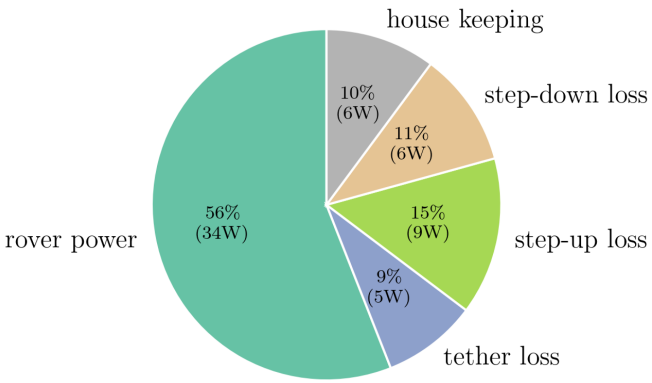

Figure 12: *Power Allocation*: This chart shows how 62 W from the lander are distributed between rover power and losses from heating and inefficiencies. We note that house-keeping power is defined at the minimal power draw to operate power conversion avionics.

Several, wired communication protocol are available for transmission over distances of 300 m. By far the fastest approach is to use fiber optics, but the problem is that fibers are not nearly as tolerant to sharp bends as compliant copper wires. We must also consider communication bottlenecks in the path from the rover to Earth. For Moon Diver, the communication bandwidth would be limited by lander to Earth transmission rates, which are on the order of 1 Mb/s between Earth and the lander. Furthermore, the average data throughput from the rover to the lander is not expected to exceed 290 kb/s. Perhaps the most important metric in selecting an appropriate protocol is the demonstration of hardware in space environments. The following table compares four common approaches, one of which has no space heritage. Given the maximum data bandwidth, the tether is less of a communication bottleneck than lander-to-Earth transmission. Therefore, we select the RS-485 protocol, which is a robust and well demonstrated communication protocol involving just two wires and an optional, ground-reference line to control voltage drift (galvanic isolation can be used to mitigate against a drifting voltage differential).

Protocol	100 m (Mb/s)	1000 m (Mb/s)	Max Dist. (km)	Heritage
Fiber	>100	>100	~10	yes
DSL (VDSL)	<100	25	5	no
RS-422	1	0.1	1	yes
RS-485	4	0.4	1	yes

Table 4: *Communication Protocol*: This table compares protocol options for tether communications.

5. Testing

For test and evaluation, several tethers were fabricated by *Falmat Custom Cable Technologies*, who provided invaluable guidance on practice design and material selection. A prototype of the Moon Diver tether is shown in Figure 1 (first page). In total, five tethers were produced with the following specifications:

Tether ID	Wire #	Wire AWG	Strength (kN)	Abrasion Material	Diam (mm)
T1	8	26	5.3	Tefzel Ext.	5.0
T2	6	28	5.3	Tefzel Ext.	4.2
T3	4	28	5.3	Tefzel Ext.	4.0
T4	4	28	5.3	PA-11 Ext.	4.0
T5	4	28	5.3	Poly Braid	4.5

Table 5: *Test Tethers*: Tethers T1 through T4 have extruded jackets while T5 has a braided Dacron (polyester) jacket.

We note that T1 is fabricated with a single-mode fiber in the center for future testing purposes; this paper does not include any results from fiber-optic testing. Also, since the tethers were received at different times in the development process, not all tethers were tested in all experiments.

Mechanical

A series of mechanical tests were performed to determine abrasion, bend, and tensile properties under simulated lunar conditions. Images from these tests are shown in Figure 13. The following table provides test results from an abrasion testbed where tethers with braided and extruded jackets were exposed to volcanic rocks under load. Braided jackets per-

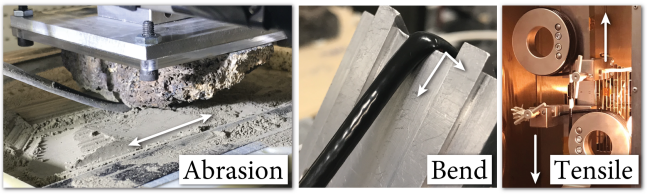

Figure 13: *Mechanical Tests*: Images from tests conducted on the tether are shown. The regolith used was fine-grain JSC-1A. The regolith exacerbates abrasion between the tether and rock and quickly tears the strength layers once exposed after hundreds of abrasion cycles.

Tether Jacket	Cycles to Fail	Tension (N)	Bend Angle	Stroke (cm/sec)	Rock Type
Braided Poly	1,557	162	174	46/1	Easy Basalt (Pahoehoe)
	1,952	162	174	46/1	Hard Basalt (A'a)
Extruded Tefzel	12,987	162	162	46/1	Easy Basalt (Pahoehoe)
	2,733	162	162	46/1	Hard Basalt (A'a)

Table 6: *Abrasion Test*: Tethers with different jackets are evaluated to determine robustness to volcanic rocks. Extruded jackets out perform braided jackets overall.

formed poorly because small tears quickly caused the braid to detach (like a rolled up sleeve), directly exposing the strength fibers below. In fact, we observed that strength fibers alone can take many more cycles of abrasion on rock than the braided jacket. However, it is not ideal to expose large areas of the strength layer as the intrusion of regolith could critically damage strength fibers. Extruded jackets did not separate even when one side was worn by abrasion, which limits the amount of potential damage through UV or regolith exposure.

Once the extruded jacket was determined to provide superior abrasion protection, tests were continued to evaluate abrasion performance under potential mission conditions (excluding vacuum and temperature). We established a simple model for abrasion that relates driven distance to abrasion cycles as shown in Figure 14. The cycles relate to the geometry of the Axel rover wheels, which have large grousers or paddles that cause oscillating motion over the terrain.

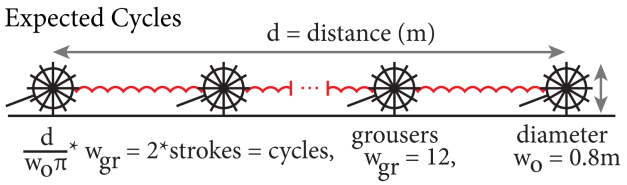

Figure 14: *Abrasion Model*: This model assumes that abrasion cycles result from oscillatory motion of the rover on the terrain. We assume that oscillations correspond directly to abrasion cycles and stroke length relates to how loaded the cable is and where in the traverse the rover is.

Field observations of the Axel rover were used to define a typical abrasion stroke, rate, and load, assuming that cycles correspond to oscillations from grousers. These parameters were then associated to a terrain type, e.g., flat surface, sloped transition, and vertical pit descent; as the rover transitions to steep terrain the load on the tether increases and the abrasion stroke length decreases due to capstaning (or friction anchoring) on the terrain. To test these parameters, an adjustable, multi-axis abrasion rig was used. The worst-case results for different tests and terrain types are shown. In all tests, a section of 4-wire, T3 tether was loaded and abraided using a combination of basalt rock and JSC-1A lunar regolith simulant. The results shown represent the worst performing

Terrain	Tension (N)	Stroke (cm/sec)	Test Cond.	CBE Cycles	Cycles to Fail
Surface	72	8/4	Basalt, JSC-1A	250	1,095
Transition	111	2/4	Basalt, JSC-1A	100	297
Pit	200	1/4	Just Basalt	300	1,160

Table 7: *Simulated Environment Abrasion Test*

trial of a series of tests involving over 20 trials with varying parameters. The CBE, or current best estimate of cycles, comes from the proposed model, which is purposely over conservative and assumes that cyclic abrasion occurs for the entire traverse and at exactly the same point along the tether. The important finding is that, even for a very conservative abrasion model, the tether outperforms the CBE.

Bend tests were performed on the tether to determine its response to sharp objects under high load. The test involved a winch system that exerted tension on a short tether segment as it was bent at a 90 degrees over a 'knife-edge' wedge. The internal wire continuity is monitored for breaks, which we report as tether failures. Table 8 shows three tests with the T3 cable, where the max tension is recorded just before a wire is severed or the tether breaks. As shown, all three tests demonstrate breaking loads over a knife-edge bend that far exceed the CBE. Next, we evaluated tensile properties under

Test 1	Test 2	Test 3	CBE
1105 N	1200 N	1215 N	200 N

Table 8: *Knife-Edge Bend Test*

lunar temperature regimes using an *Instron* machine with attached thermal chamber. The test slowly pulled tension on tether segments, which were mounted to capstan anchors inside the chamber. The chamber is brought to temperature prior to testing. The results reported in the following table show tether performance at expected max/min temperatures. The T1 tether was used for all tests. We also note that some samples from the thermal-vacuum, sun-simulator test (described in Section 5) were tested to evaluate post-exposure performance. In all hot tests, tethers performed slightly worse than the manufacturers rated load (5.3 kN). In cold tests, the tethers tensile strength increased significantly. This result is expected and has been reported for Vectran and other high-strength materials; as temperature decreases the tensile strength increases [16]. In all cases, the tether's strength was better than the CBE static load requirement by a factor of 20 to 40 depending on the temperature.

Condition	Break (kN)	Temp (C)	UV Exp.
Pristine	4.1	150	
	4.27	150	
	10.28	-50	
	8.54	-50	X
Mild Abrasion	3.2	150	X
	3.14	150	X
Heavy Abrasion	3.38	150	

Table 9: *Thermal Tensile Tests*

Electrical:

We performed a combined communication/power test using a 477 m continuous segment of T3 tether. The setup and result are indicated in Figure 15. The test involved two wire pairs,

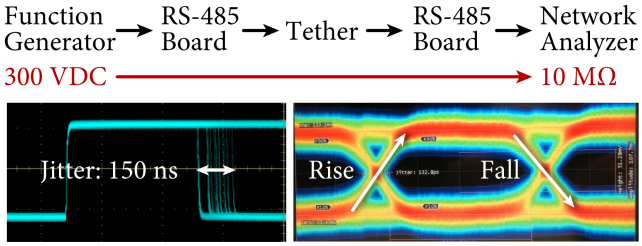

Figure 15: *Power/Communication Test*: The test setup/flow is illustrated above the images, which show ideal, eye-diagram patterns using RS-485 at 3 Mb/s over a 477 m tether.

one dedicated for RS-485 communications, the other for power. The communications test used a function generator to drive a Linear Technologies RS-485 development board. The signal passed through the tether while 300 VDC was run on a separate adjacent pair without noticeable impact. Two custom breakout boards where attached to either end of the tether. On the receiving end, the signal was decoded by a second RS-485 board and read by a network analyzer to create the signal jitter and eye diagram shown in Figure 15. As shown, the signal, which was driven at various frequencies over 500 m, exhibits negligible jitter (150 ns) and an ideal eye-diagram. The performance of the RS-485 approach is viable up to ~3 Mb/s, after which the signal is more noisy. We note that, with improvements to impedance matching and termination design, we could achieve greater speeds. However, the tested speed is already 15 times faster than that required by the mission.

Environmental

As mentioned, we performed a thermal-vacuum test with simulated sunlight on eight test tethers with varying degrees of abrasion. The tests were performed by Lockheed Martin in Palo Alto, California. The chamber pressure was brought to $1x10^{-5}$ Torr and samples were placed on a thermal plate heated to 145 C for 72 hours. A sun simulator was operated at five times strength to mimic full-spectrum (AMO) UV degradation over the course of an expected 15 day mission. The test setup, UV beam, and tether samples are shown in Figure 16. We performed visual post analysis on the tethers and observed characteristic yellowing of exposed strength fibers and no change in pristine, non abraided, tethers. Some samples were sent for tensile testing and showed no noticeable strength loss in comparison to similarly-abraided, non-exposed tethers. The remaining tethers have been stored for more detailed material testing at a later date.

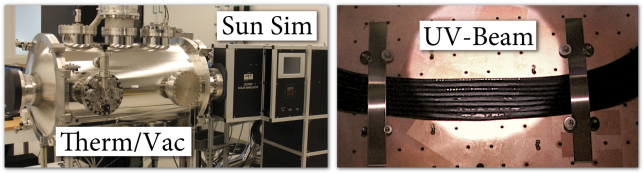

Figure 16: *Thermal Vacuum and UV Test*: The internal and external chamber are shown along with the pre and post exposed tether articles. The sun simulator allows for full-spectrum UV light to shine on the samples over three days at five times sun power.

Figure 17: *Field Test*: Images from an Axel rover field test in Arizona are shown. The tether was mildly abraided by basalts at discrete points along the tether. However, the abrasion jacket remained in tact and showed only light scrapping.

Field

Finally, we integrated a T3 tether into the Axel rover and conducted three field experiments at different sites: Devolites Crater in Arizona, Gold Queen Mine and Fossil Falls in Mojave, California. Images from these tests are shown in Figure 17. In all tests the tether performed well and only showed minor abrasion to the jacket with small jacket cuts occurring only after multiple field and on-lab tests. To understand the loads on the tether in more detail, we used a load cell mounted to the anchor of the tether during our field test to Devolites Crater. The tension was recorded and is plotted in Figure 18. The biggest takeaways from testing the tether in the field are that 1) the taut tether forms a nearly perfect, straight line from the anchor to the terrain or end

of Axel's tether boom, and 2) cyclic abrasion occurs due to the rover's oscillating motion over the terrain and imprecise tension management. Abrasion can thus be reduced by tuning tension control and looking at alternative wheel geometries suited for the lunar terrain.

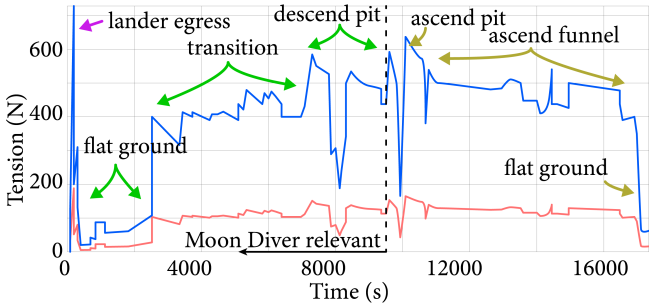

Figure 18: *Lander Tension*: The following plot shows the output of a tension sensor placed in line with the tether anchor during the Arizona field test. Tension is tracked starting from lander egress, where the rover is fully suspended as it lowers itself from the lander deck (1 m up) down to the surface. Next, the rover drives a 100 m path to the entrance of a vertical pit. Once on the transition into the pit, the tension increases. The dotted line shows the end point of Axel's descent into the pit, which would represent the Moon Diver operational scenario. The tension during the ascent is provided for reference only. The plot is labeled and shows the actual tension (blue) and the estimated lunar tension (red). The estimated tension simply divides the actual by a factor of 6 to adjust for gravity differences between the Moon and Earth. Since the tether is in contact with the terrain near the pit transition, the tension sensed at the anchor is likely lower than that on the rover. This study did not include measurements from the Axel rover because the output of its load cell was uncalibrated and only available as a voltage. The takeaway is that the tension does not exceed the rated strength of the tether even for Earth use.

6. Conclusion

This paper presents a design trade and test analysis for a lunar electromechanical, rover tether. This work advances the design of the Axel tether to reduce the risk associated with rappelling on a rugged lunar surface by tailoring the tether's mechanical structure and electrical properties to meet mechanical support, power, and wired communications requirements. With respect to strength, we show a design that can both support a suspended rover and is robust to terrain contacts. With respect to power, we show analysis of loss and consider a range of voltages and wire thicknesses that allow for the transmission of over 50 W across a 300 m tether. Our communications approach has been tested to allow 3 Mb/s transmission across a long cable using the high-heritage, RS-485 protocol. Finally, we present a series of mechanical, electrical, and environmental tests that demonstrate the capability of the tether to perform in a harsh lunar environment.

Acknowledgments

This research was carried out at the Jet Propulsion Laboratory, California Institute of Technology, under a contract with the National Aeronautics and Space Administration. The information presented about the Moon Diver mission concept is pre-decisional and is provided for planning and discussion purposes only. We would also like to thank the following organizations for their help in design and testing: Falmat Tethers for design guidance and fabrication of multiple prototype tethers, North Eastern University Capstone Team for providing an abrasion testbed to assist in testing efforts, and Lockheed Martin for assistance with UV testing.

References

[1] L. Kerber, I. Nesnas, L. Keszthelyi, J. Head, B. Denevi, P. Hayne, K. Mitchell, J. Ashley, J. Whitten, A. Stickle *et al.*, "Moon Diver: A Discovery mission concept for understanding the history of the mare basalts through the exploration of a lunar mare pit," in *New Views of the Moon 2-Asia*, vol. 2070, 2018.

[2] I. A. Nesnas, L. Kerber, A. Parness, R. Kornfeld, G. Sellar, P. McGarey, T. Brown, M. Paton, M. Smith, A. Johnson *et al.*, "Moon Diver: A Discovery Mission Concept for Understanding the History of Secondary Crusts through the Exploration of a Lunar Mare Pit," in *2019 IEEE Aerospace Conference*. IEEE, 2019, pp. 1–23.

[3] J. Haruyama, K. Hioki, M. Shirao, T. Morota, H. Hiesinger, C. H. van der Bogert, H. Miyamoto, A. Iwasaki, Y. Yokota, M. Ohtake *et al.*, "Possible lunar lava tube skylight observed by SELENE cameras," *Geophysical Research Letters*, vol. 36, no. 21, 2009.

[4] M. Robinson, J. Ashley, A. Boyd, R. Wagner, E. Speyerer, B. R. Hawke, H. Hiesinger, and C. Van Der Bogert, "Confirmation of sublunarean voids and thin layering in mare deposits," *Planetary and Space Science*, vol. 69, no. 1, pp. 18–27, 2012.

[5] I. A. Nesnas, P. Abad-Manterola, J. A. Edlund, and J. W. Burdick, "Axel mobility platform for steep terrain excursions and sampling on planetary surfaces," in *IEEE Aerospace Conference*. IEEE, 2008, pp. 1–11.

[6] I. A. Nesnas, J. B. Matthews, P. Abad-Manterola, J. W. Burdick, J. A. Edlund, J. C. Morrison, R. D. Peters, M. M. Tanner, R. N. Miyake, B. S. Solish *et al.*, "Axel and DuAxel rovers for the sustainable exploration of extreme terrains," *Journal of Field Robotics*, vol. 29, no. 4, pp. 663–685, 2012.

[7] Y. Chen, R. Huang, X. Ren, L. He, and Y. He, "History of the tether concept and tether missions: a review," *ISRN astronomy and astrophysics*, vol. 2013, 2013.

[8] M. Dobrowolny and N. Stone, "A technical overview of tss-1: the first tethered-satellite system mission," *Il Nuovo Cimento C*, vol. 17, no. 1, pp. 1–12, 1994.

[9] T. A. Sullivan, "Catalog of Apollo experiment operations," 1993.

[10] M. J. Gradziel and K. J. Holgerson, "Mechanisms for lowering tethered payloads: lessons learned from the mars exploration program," in *2008 IEEE Aerospace Conference*. IEEE, 2008, pp. 1–20.

[11] C. Krause, C. Fantinati, E. Barrett, M. Grott, T. Hudson, S. Jansen, J. Jänchen, J. Knollenberg, O. Küchemann, D. May *et al.*, "HP3–Experiment on InSight Mission–Operations on Mars," in *2018 SpaceOps Conference*, 2018, p. 2347.

[12] D. Wettergreen, C. Thorpe, and R. Whittaker, "Exploring Mount Erebus by walking robot," *Robotics and Autonomous Systems*, vol. 11, no. 3-4, pp. 171–185, 1993.

[13] T. Huntsberger, A. Stroupe, H. Aghazarian, M. Garrett, P. Younse, and M. Powell, "TRESSA: Teamed robots for exploration and science on steep areas," *Journal of Field Robotics*, vol. 24, no. 11-12, pp. 1015–1031, 2007.

[14] P. McGarey, F. Pomerleau, and T. D. Barfoot, "System design of a tethered robotic explorer (TReX) for 3D mapping of steep terrain and harsh environments," in *Field and Service Robotics*. Springer, 2016, pp. 267–281.

[15] D. Schmucking, M. Schenk, and A. Worner, "Crosstalk cancellation for hybrid fiber twisted-pair systems," in *Proceedings of GLOBECOM'96. 1996 IEEE Global Telecommunications Conference*, vol. 2. IEEE, 1996, pp. 783–787.

[16] J. Stein, C. Sandy, D. Wilson, G. Sharpe, and C. Knoll, "Recent developments in inflatable airbag impact attenuation systems for mars exploration," in *44th AIAA/ASME/ASCE/AHS/ASC Structures, Structural Dynamics, and Materials Conference*, 2003, p. 1900.

BIOGRAPHY

Patrick McGarey *Ph.D. is a Robotics Technologist at JPL in the Robotic Mobility Group. Patrick received his Ph.D. in Aerospace Engineering from the University of Toronto, where he was a visiting Fulbright Scholar. His research is focused on the development of tethered systems and autonomy functions for the exploration of extreme environments throughout the solar system.*

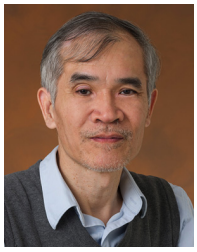

Tien Nguyen *is a JPL Fellow with a B.S. in Physics, Electrical Engineering and Mechanical Engineering, and an M.S. with a double major in Electrical Engineering and Mechanical Engineering. Tien has worked on numerous tiger teams for several of JPL's high profile space flight missions such as Galileo, Magellan, Cassini, MER, Dawn and MSL.*

Torkom Pailevanian *is a robotics engineer in the Robotic Actuation and Sensing group at JPL. He received his BS and MS from Caltech, where he worked on the development of biodevices for cancer treatment and autonomous underwater robotics systems. He is currently supporting the system architecture, circuit design and firmware tasks for extreme environment robotics.*

Issa Nesnas *Ph.D. is a principal technologist and the supervisor of the Robotic Mobility group at the Jet Propulsion Laboratory with over two decades of research in space robotics and industrial automation. He is the principal investigator for the Axel robot and leads research in autonomy and mobility with a focus on extreme terrain access and micro-gravity mobility.*